JKAU: Met., Env. & Arid Land Agric. Sci., **Vol. 17** No. 2, pp: 87-102 (2006 A.D. / 1427 A.H.)

Ultraviolet-B Radiation Forecast over Aswan

H. Abdel Basset and M.H. Korany*

Dept. of Meteorology, Faculty of Met., Env. and Arid Land Agric.
King Abdulaziz University, Jeddah, Saudi Arabia
**Egyptian Meteorological Authority, Cairo, Egypt*

Abstract. This work aimed to forecasting UV-B radiation over Aswan (32.78ºE, 23.97ºN) by deducing an empirical formula relating UV-B radiation with the global solar radiation and the total amount of ozone. The UV-B radiation forecast was produced in three steps. First, total ozone was estimated over Aswan using a regression relationship between the thickness of two atmospheric layers and total ozone. Second, the residual method was used to deduce a formula relating the global solar radiation with surface atmospheric variables. Finally, the total ozone and global solar radiation were fed into the formula to obtain the UV-B radiation forecast. The above steps were applied on the four seasons and also on the annual values. The highest strong correlation occurred at autumn and winter for ozone while at spring and autumn for global solar radiation.

1. Introduction

Recent changes in the stratospheric ozone levels have attracted strong interest from the scientific and environmental communities as well as from policy makers. The most significant influence on received clear-sky UV-B radiation is that resulting from variation in atmospheric ozone (Frederick, *et al*., 1993). This is very important especially when the ozone column has a downward trend in extratropical latitudes (Bojkov, *et al*., 1990). UV-B radiation levels at the Canadian border have increased 4% per decade. At 55º degrees south latitude an increase in UV-B radiation level of 9.9% per decade has been recorded over the last 15 years.

The amount of UV-B radiation received at the ground level depends on various temporal, spatial and meteorological factors such as time of the day, season, latitude, altitude, clouds, surface albedo, ozone, air particulates and aerosols (Frederick, *et al*., 1993). Any small increase in UV-B radiation flux could be

offset by other competing factors. In fact, some studies (Berger and Urbach, 1982 and Scotto, *et al*., 1988) have shown lower levels of UV-B radiation reaching the ground. These decreases have been attributed to scattering and absorption by pollutant gases and dust particles (Grant, 1988) and also tropospheric ozone. The atmospheric parameters strongly affect UV-B radiation values measured at the surface of the earth.

It is known that the daily total ozone amount (Ω) is linked with meteorological features and this correlation has been appreciated since the beginning of research on atmospheric ozone. The nature of day-to-day total ozone fluctuations has been of considerable interest for many years. Significant statistical relations between Ω and a number of meteorological variables have long been known (*e.g*., Dobson, *et al*., 1929; Reed, 1950; Normand, 1953; Vaughan and Price, 1991; Abdel Basset and Gahein, 2000 & 2003) and have recently been used in short-term Ω forecasting in middle and high latitudes (Burrows *et al*., 1993, 1994; Poulin and Evans, 1994; Austin, *et al*., 1994 and Vogel, *et al*., 1995). These statistical relations are, however, regionally and seasonally variable in their strengths (Ohring and Muench, 1960; Schubert and Munteanu, 1988; Mote, *et al*., 1991 and Petzoldt, *et al*., 1994).

Early studies based on a limited number of ground station reports (Dobson, *et al*., 1929) helped to establish a firm meteorological basis for the observed daily ozone variation. Reed (1950) pointed out that ozone variations are not only caused by chemical processes but also have dynamical origins, expressed by sudden increases in total ozone accompanying marked increase in tropopause pressure, such as found during the passage of a cold front or depression. This can be interpreted simply as an increase in the depth of ozone and the ozone-rich stratosphere or as a combination of vertical and horizontal advection of ozone.

Ozone absorbs most of the harmful ultraviolet radiation emitted by the sun before it reaches the earth's surface. This absorption creates a heat source, which leads to a heating layer in the atmosphere producing temperature increases with height (stratosphere). The laboratory of atmospheric physics at the University of Thessaloniki provides an approach used for regional ozone forecasting (Vogel, *et al*., 1995). This approach is based on results from detailed statistical calculations showing strong correlation between Ω and meteorological parameters in the lower stratosphere and higher troposphere. From this point of view we can use the thermal structure of the atmosphere in the ozone forecasting technique. Ozone is found in two different height regions in the atmosphere at heights between about 10 and 50 km in the stratosphere while the remaining ozone is found closer to the surface in the troposphere. The aim of this study is to forecast the UV-B radiation from the global solar radiation and the total amount of ozone at Aswan (32.78ºE, 23.97ºN).

2. Data and Methodology

2.1. Stratospheric Ozone Measurements in Egypt

A global network of ozone observing stations formed part of the plans for the ambitious International Geophysical Year (IGY) of 1957. During the IGY year, WMO assumed responsibility for the collection of ozone data. In collaboration with the International Ozone Commission, the Organization developed standard procedures and coordination, thereby ensuring uniform high quality ozone measurements. As early as October 1967, the Egyptian Meteorological Authority (EMA) introduced regular monitoring of ozone at Cairo using the Dobson Spectrophotometer No. 96. In 1973 Cairo became the Regional Ozone Center (ROC) for ozone stations in North Africa and the Middle East. The role of ROC was to study the variation of ozone over Egypt. Therefore, EMA at the end of 1984 started to measure ozone amount over Aswan (Upper Egypt) by Dobson Spectrophotometer No. 69. To study the effect of South European Ozone (SEO) for Egypt, EMA measured ozone by Brewer Spectrophotometer No. 143 over Mersa Matruh (coastal station) in November 1998. Because the situation of ozone over the Red Sea area was unclear, WMO and EMA started to measure the total amount of ozone over Hurghada (GAW station) by Dobson spectrophotometer No. 59 from November 2000. Table 1 illustrates the locations, WMO numbers and ozone ID numbers of the four ozone stations. The instruments have been maintained in good condition and we get high quality ozone data that are needed not only for long-term monitoring but also in forecasting technique of UV-B radiation.

Table 1. The Egyptian ozone stations.

	Cairo	**Aswan**	**Matruh**	**Hurghada**
WMO No.	62371	62414	62306	62464
Ozone ID.	152	245	376	409
Latitude	30.08ºN	23.97ºN	31.33ºN	27.28ºN
Longitude	31.28ºE	32.78º · E	27.22ºE	33.75ºE
Height (meter)	037	193	035	007
Instrument	Dobson # 096	Dobson # 069	Brewer # 143	Dobson # 059
Elements	O_3	O_3	O_3, UV-B	O_3
Started at	October 1967	December 1984	November 1998	November 2000
Last calibration	Germany, 2001	Swiss, 1999	–	Germany, 2000

2.2 ECMWF Data

Meteorological data used in this study have been taken from the archives of the European Center for Medium Range Weather Forecasts (ECMWF). The data consist of the geopotential heights (Z) on regular latitude-longitude grid points with resolution of 2.5º × 2.5º. The data are only available at 1200 UTC during the period 1986 to 1989 at isobaric levels 1000, 850, 700, 500, 400, 300, 250, 200, 150 and 100 hPa. The geopotential height over Aswan was obtained by interpolation.

2.3 Residual Method

The success of a statistical forecasting method does, to some extent depend on the technique applied, but it depends even more on the selection of the predictors. After choosing a number of predictors from the physical point of view, the problem is what is the best method to be used ? One method of doing this is by using them one by one in a successive correction manner. In this case we start with the best of these predictors. The residual method has been applied to explore the possibility of forecasting total ozone values by means of atmospheric thicknesses of different layers. The value of Ω during the period of study for each station has been taken as the dependent variable (predictand) and the corresponding values of the thicknesses of different layers were the independent variables (predictors).

First Step. The correlation coefficient (r) between the values of total ozone and the thickness of different layers (predictors) has been estimated. The predictor having the strongest (r) with the predictand was used as the first predictor, and then the regression line and the regression coefficients were determined. Then the error between the actual and estimated values of total ozone was taken as a predictand.

Second Step. The above mentioned error was subjected to the process performed in the first step. The second step was then repeated with new predictors (if many) until the additional predictor had no significant effect on the predictand and there was no need for any further iteration steps (*i.e.*, the improvement could not be expected to be very great with adding new predictors). This method has been applied at Aswan and provides five equations (one equation for each season and the fifth represents the annual variation).

3. Estimation of Daily Total Ozone Aamount (Ω)

In this section, the relationship between Ω and the depth intervals between geopotential heights (the thicknesses of different layers of the atmosphere) at Aswan will be investigated. The method is based on the assumption that short-

term variation of total ozone content can be brought into an empirical relation with thermal structure of the atmosphere, namely, with short-term variations of tropospheric and stratospheric temperature. We investigated the relation between Ω and the thickness of two layers ΔZ1 and ΔZ2, where ΔZ1 is the height difference between 500 hPa and 1000 hPa and ΔZ2 is the height difference between 100 hPa and 200 or 300 hPa. The strong relationship between Ω, ΔZ1 and ΔZ2 was used to deduce a linear regression equation relating the above parameters. We used the residual method to deduce such a relationship, which was applied to the seasonal and annual data.

The daily values of four years of geopotential height from the ECMWF data with the actual measurements of Ω have been used to deduce five equations to estimate Ω at Aswan (Table 2). The last equation (1e) represents the daily values for all the year while the other four equations (1a-1d) represent the four seasons.

Table 2. Aswan regression coefficients (A_i, B_i) of Ω estimation, MAE, RMSE, and R from a stepwise regression analysis during: (a) winter, (b) spring, (c) summer, (d) autumn, and (e) for the annual data.

a) Winter

Step no.	ΔZ	Regression coefficients		MAE	RMSE	R
		A_i	B_i			
1	500-1000	733.056	–0.08336	9.7527	12.4154	–0.46
2	100-500	936.2444	–0.08763	9.3011	12.0145	0.61

$$\Omega = 1669.3004 - 0.08336 * Z(500\text{-}1000) - 0.08763 * Z(100 - 500) \quad (1a)$$

b) Spring

Step no.	ΔZ	Regression coefficients		MAE	RMSE	R
		A_i	B_i			
1	500-700	717.0259	–0.16143	11.1951	14.3955	–0.3
2	100-300	665.3124	–0.24485	10.5451	13.2608	0.5

$$\Omega = 1382.3383 * 0.16143 * Z(500\text{-}700) - 0.24485 * Z(200 - 300) \quad (1b)$$

c) Summer

Step no.	ΔZ	Regression coefficients		MAE	RMSE	R
		A_i	B_i			
1	500-1000	741.1255	–0.07762	6.9683	8.7716	–0.3
2	100-500	609.8589	–0.05633	6.6506	8.4029	0.58

$$\Omega = 1350.9844 - 0.07762 * Z(500\text{-}1000) - 0.05633 * Z(100 - 500) \quad (1c)$$

Table 2. Contd.

d) Autumn

Step no.	ΔZ	Regression coefficients		MAE	RMSE	R
		A_i	B_i			
1	500-1000	–333.5746	0.10351	5.8274	7.3449	0.62
2	100-300	–67.3821	0.00972	5.8002	7.3390	0.75

$$\Omega = -400.9567 + 0.10351 * Z(500\text{-}1000) + 0.00972 * Z(100 - 300) \quad (1d)$$

e) Annual

Step no.	ΔZ	Regression coefficients		MAE	RMSE	R
		A_i	B_i			
1	500-1000	–159.6035	0.07504	11.5462	14.4819	0.46
2	100-300	–522.9647	0.07528	11.1586	14.1015	0.65

$$\Omega = -682.5682 + 0.07504 * Z(500\text{-}1000) + 0.07528 * Z(100 - 300) \quad (1e)$$

Table 2 shows the number of steps, the predictor used in each step, the regression coefficients arising in each step (A_i, B_i), the mean absolute error (MAE) and root mean square error (RMSE) arising from the error between the actual and estimated data after each step, and multiple correlation coefficient (R) from a stepwise regression analysis. It is clear that two predictors have been used to reach a reasonable total multiple correlation values for the four seasons and the annual variation. The highest value of the total multiple correlations appeared in autumn.

We applied the five deduced equations (1a-1e) to estimate Ω for the period from 1 January to 31 December 2000, for which the measured Ω were available on a daily basis. Figure 1 shows the actual and estimated values of Ω during this period, while Fig. 2 illustrates the measured and estimated values of Ω for the four seasons. Generally, the best agreement between the actual and estimated values of Ω occurs in summer and autumn seasons. Also a good agreement between the actual and estimated values of Ω appears with the annual values except during October and November (Fig. 1).

4. Estimation of Daily Global Solar Radiation (G)

The daily global solar radiation (G) at the Earth's surface is a function of meteorological variables. So, it can be estimated using data of routine meteorological observations such as mean, maximum, and minimum surface temperature (T_{mean}, T_{max}, and T_{min}), daily mean relative humidity (RH), cloud amount (CLD) and daily mean surface atmospheric pressure (PRESS). Here, we

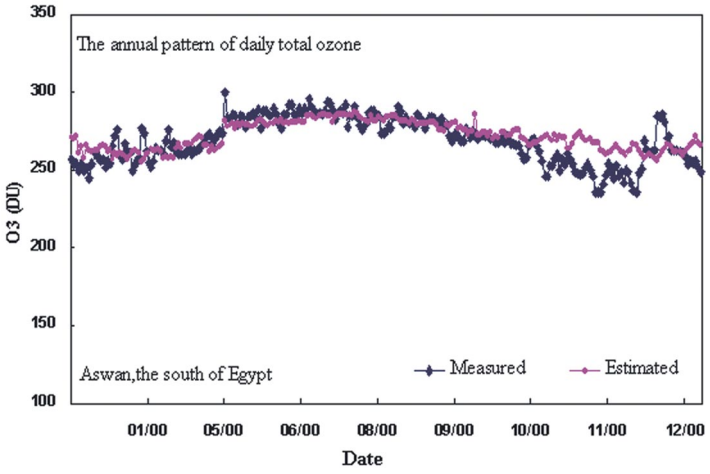

Fig. 1. Measured and estimated Ω at Aswan during 2000.

will deduce a statistical regression equation relating the global solar radiation G (as dependent variable) to the above meteorological variables (as independent variables).

We used also the residual method in forecasting the global solar radiation (G) by means of the various surface observations. The values of G during the period of study have been taken as the dependent variable (predictand) and the other variables (RH, CLD, PRESS, T_{max}, T_{min}, and T_{mean}) as predictors. Since there are significant differences between observed G in different seasons, we developed five separate regressions, one representing the annual G and the others representing that of the four seasons. The present study is based on the four most important daily data to get the five regression equations.

Table 3 shows the number of steps (the number of predictors), the regression coefficients arising in each step (A_i, B_i), the mean absolute error (MAE) and the root mean square error (RMSE) arising from the error between the actual and estimated data after each step, and multiple correlation coefficient (R) from a stepwise regression analysis. The results are illustrated in Table 3 and Fig. 3 where we found the following:

– Good agreement exists between the actual and estimated annual values of G (Fig. 3), where the total multiple correlation reached 0.83 after using four predictors. The highest values of G over Aswan occurred in the summer season.

– In winter, although we start with small R (–0.45) with the first predictors RH, we reached a reasonable total multiple correlation value (0.699) after using the four predictors.

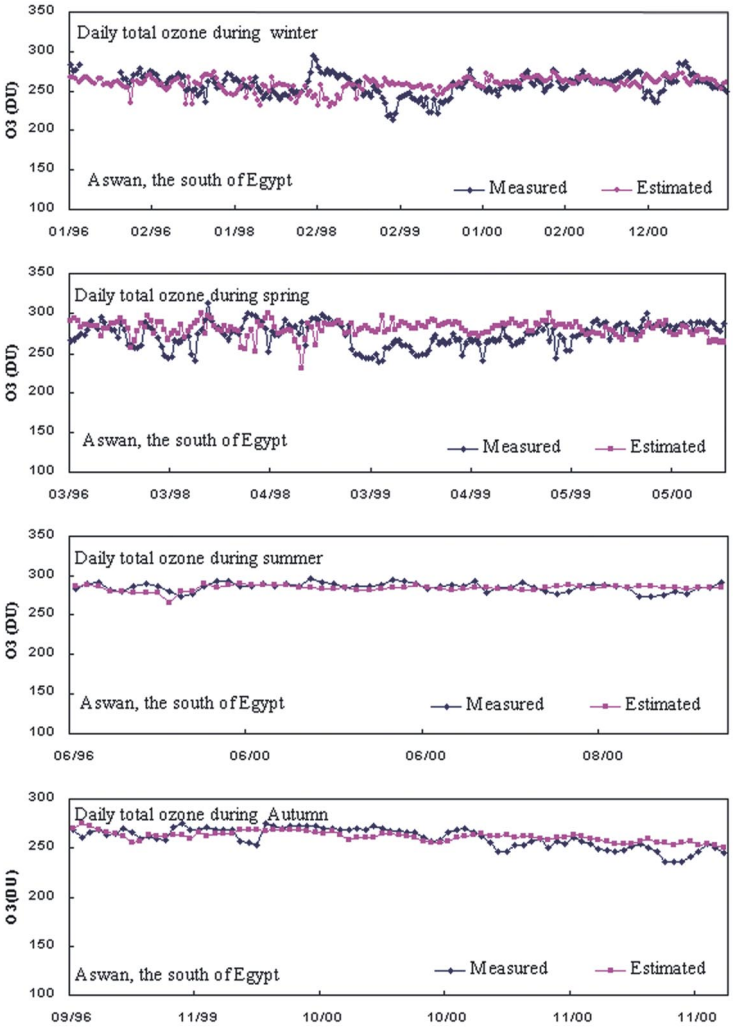

Fig. 2. Measured and estimated Ω at Aswan during the different seasons.

Table 3. Aswan regression coefficients (A_i, B_i) of (G) estimation, MAE, RMSE, and R from a stepwise regression analysis during: (a) winter, (b) spring, (c) summer, (d) autumn, and (e) for the annual data.

(a) Winter

Step no.	Predictors	Regression coefficients		MAE	RMSE	R
		A_i	B_i			
1	RH	23.50082	–0.16158	1.7637	2.2167	–0.45
2	CLD	0.75657	–0.98957	1.5431	1.8876	–0.52
3	PRESS	–159.9828	0.16091	1.5243	1.8292	0.625
4	T_{max}-T_{min}	–1.09058	0.08274	1.5124	1.8201	0.699

$$G = -136.81599 - 0.16158 * RH - 0.98957 * CLD + 0.16091 * PRESS + 0.08274 * (T_{max} - T_{min}) \quad (2a)$$

(b) Spring

Step no.	Predictors	Regression coefficients		MAE	RMSE	R
		A_i	B_i			
1	CLD	26.65243	–1.51004	1.9966	2.6661	–0.68
2	RH	4.74032	–0.2062	1.6747	2.3267	–0.704
3	T_{mean}	–0.99396	0.03901	1.6649	2.3154	0.742
4	PRESS	–83.23336	0.08413	1.6492	2.2944	0.783

$$G = -52.83457 - 1.51004 * CLD - 0.2062 * RH + 0.03901 * T_{mean} + 0.08413 * PRESS \quad (2b)$$

(c) Summer

Step no.	Predictors	Regression coefficients		MAE	RMSE	R
		A_i	B_i			
1	CLD	27.8362	–0.9285	1.0343	1.3104	–0.44
2	T_{mean}	9.14503	–0.2659	0.9419	1.2111	0.498
3	RH	2.94426	–0.15168	0.8632	1.0995	0.592
4	PRESS	–40.5999	0.04124	0.86	1.0967	0.67

$$G = -0.67441 - 0.9285 * CLD - 0.2659 * T_{mean} - 0.15168 * RH + 0.04124 * PRESS \quad (2c)$$

(d) Autumn

Step no.	Predictors	Regression coefficients		MAE	RMSE	R
		A_i	B_i			
1	T_{mean}	6.41325	0.50103	1.6533	2.0029	0.78
2	CLD	0.54622	–1.26147	1.4307	1.7017	0.804

Table 3. Contd.

(d) Autumn

Step no.	Predictors	Regression coefficients		MAE	RMSE	R
		A_i	B_i			
3	PRESS	45.43114	–0.04594	1.4226	1.6958	0.82
4	RH	–0.16302	0.00583	1.4205	1.6949	0.86

$$G = 52.22759 + 0.50103 * T_{mean} - 1.26147 * CLD - 0.04594 * PRESS + 0.00583 * RH \quad (2d)$$

(e) Annual

Step no.	Predictors	Regression coefficients		MAE	RMSE	R
		A_i	B_i			
1	RH	32.23647	–0.35907	2.4694	3.1366	–0.77
2	CLD	0.70514	–0.98547	2.2880	2.9060	–0.78
3	PRESS	168.3881	–0.17038	2.1727	2.8265	0.803
4	T_{max}-T_{min}	1.97953	–0.14135	2.1605	2.8071	0.825

$$G = 203.30924 \quad 0.35907 \quad RH \quad 0.98547 \quad CLD \quad 0.17038 \quad PRESS + 0.14135\ (T_{max}\text{-}T_{min}) \quad (2d)$$

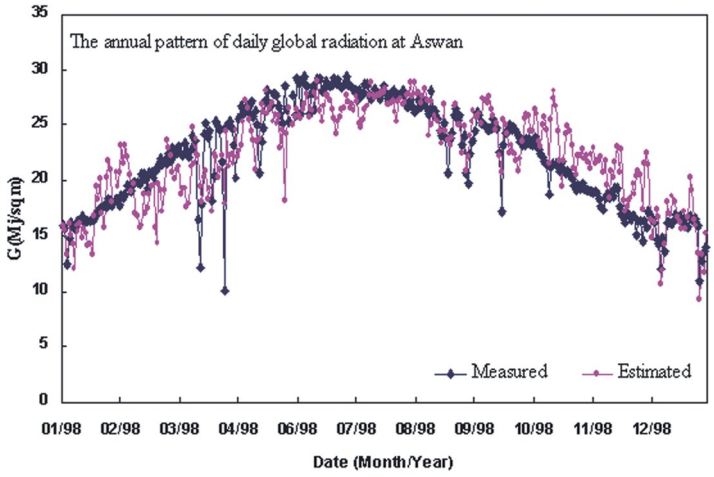

Fig. 3. Measured and estimated daily total global radiation at Aswan during 1998.

– For autumn, the total multiple correlations reached 0.86 after using four predictors. A similar high value of the total multiple correlation also appeared clear in Fig. 4, where a good agreement between the two time series is observed.

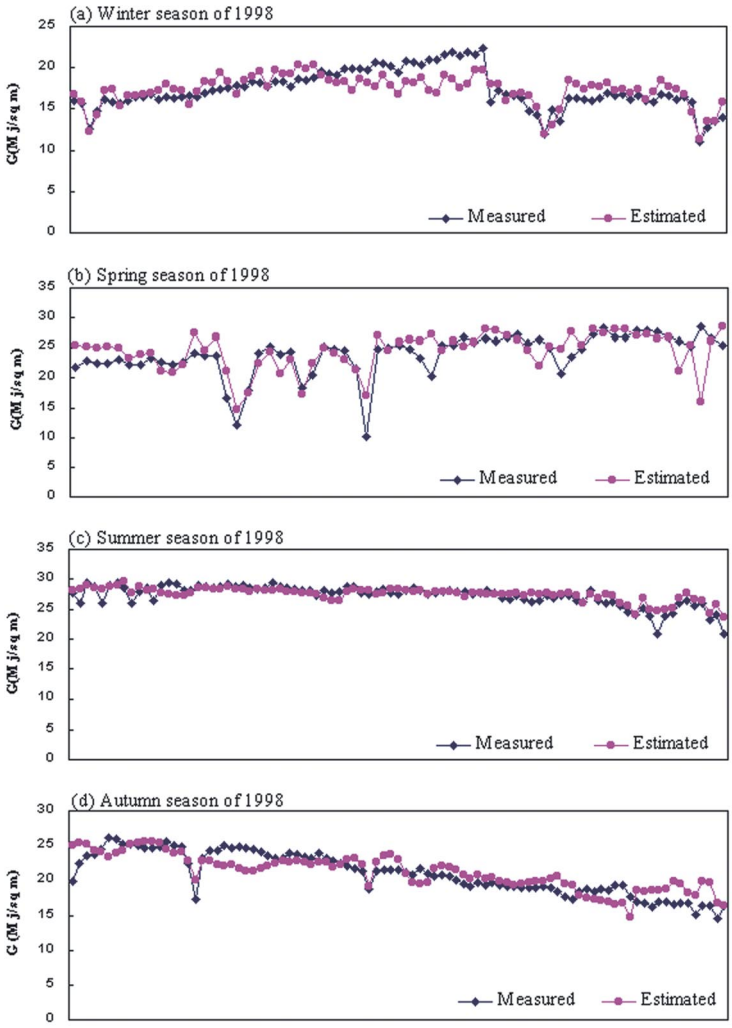

Fig. 4. Measured and estimated G at Aswan through the different season.

Equations 2a to 2e illustrate the multiple regression equations for the four seasons and the last one for the annual pattern. They were applied on another separate period of data to evaluate their accuracy. Figure 3 shows the actual and estimated daily global solar radiation for 1998. It also illustrates that the es-

timated values of the daily total global radiation are more variable than the actual values. This difference (fluctuations) between actual and estimated data are not found in Fig. 4, which means that it is better to deduce the global solar radiation from the seasonal equations than the annual equation. Figure 4 shows a good agreement between actual and estimated values of G for the four seasons especially in summer.

5. Estimation of Daily UV-B Irradiance

The documented strong relation between UV-B radiation and global solar radiation and also with ozone, enabled us to deduce an equation relating UV-B radiation with G and Ω. In this section we applied the residual method to obtain an empirical formula deducing UV-B radiation (dependent variable) from G and Ω (independent variables). Table 4 shows the number of predictors, the regression coefficients arising in each step (A_i, B_i), the MAE and RMSE between the actual and estimated data after each step, and multiple correlation coefficient (R) from a stepwise regression analysis. It is clear that the total multiple correlations reached values of 0.8 or more in the four seasons via our two predictors (G and Ω). The highest total multiple correlation occurs in autumn (0.95) which is quite high, so it is associated with lowest MAE and RMSE (0.002 and 0.00267).

Table 4. Aswan regression coefficients (A_i, B_i) of daily UVB radiation estimation, MAE, RMSE, R from a stepwise regression analysis during: (a) winter, (b) spring, (c) summer, and (d) autumn.

(a) Winter

Step no.	Predictors	Regression coefficients		MAE	RMSE	R
		A_i	B_i			
1	Global	–0.00963	0.00283	0.00308	0.00413	0.872
2	Ozone	0.02838	–0.00011	0.00291	0.00384	0.889

$$UVB = 0.01875 + 0.00283 * G - 0.00011 * \Omega \quad (3a)$$

(b) Spring

Step no.	Predictors	Regression coefficients		MAE	RMSE	R
		A_i	B_i			
1	Ozone	0.04004	0.00012	0.0079	0.00946	0.672
2	Global	–0.08238	0.00318	0.0037	0.00468	0.88

$$UVB = -0.04234 + 0.00318 * G + 0.00012 * \Omega \quad (3b)$$

Table 4. Contd.

(c) Summer

Step no.	Predictors	Regression coefficients		MAE	RMSE	R
		A_i	B_i			
1	Ozone	0.04993	0.00011	0.0005	0.0075	0.54
2	Global	–0.0673	0.0024	0.0037	0.0063	0.80

$$UVB = -0.01737 + 0.0024 * G + 0.00012 * \Omega \quad (3c)$$

(d) Autumn

Step no.	Predictors	Regression coefficients		MAE	RMSE	R
		A_i	B_i			
1	Global	–0.01989	0.00347	0.0023	0.0028	0.943
2	Ozone	–0.00374	0.00001	0.0022	0.00267	0.954

$$UVB = -0.02363 + 0.00347 * G + 0.00001 * \Omega \quad (3d)$$

Equations 3a-3d represent the obtained empirical formulae to deduce UV-B radiation for each season. We applied these equations on discrete periods of data during different seasons to verify them. Very good agreement between the actual and estimated values of UV-B radiation occurs at the different seasons as shown in Fig. 5.

7. Summary

The relationships between ozone content and the thicknesses of two different layers in the troposphere have been investigated for a period of four years. We found that there is strong correlation between ozone and the thickness of layers for the four seasons and the annual values.

The residual method has been used to evaluate linear regression equations relating the total amount of ozone to the thicknesses during the four seasons and for the annual cycle. These equations were applied to another period and promising results were found, which enable estimating the amount of ozone from the two thicknesses. Also, we deduced five regression equations relating the global solar radiation with some meteorological variables. The obtained regression equations for ozone and global solar radiation were used to deduce empirical formulas to forecast UV-B radiation from ozone and global solar radiation.

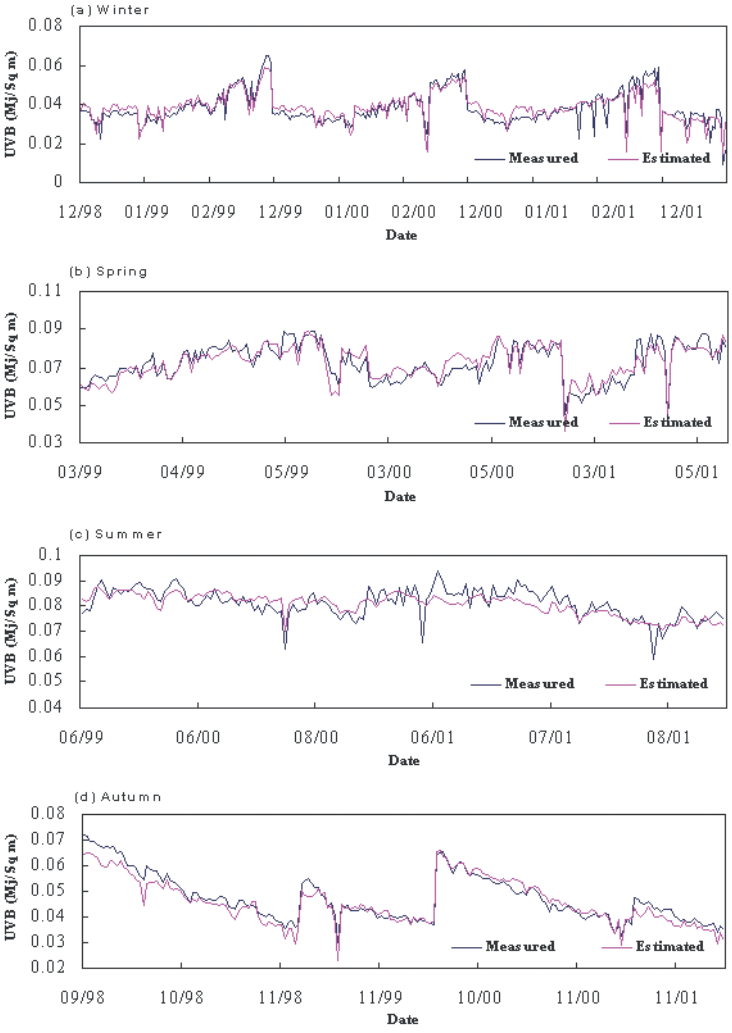

Fig. 5. Measured and estimated daily UVB radiation at Aswan through the different season.

References

Abdel Basset, H. and **Gahein, A.** (2000) On the relationship between ozone and cyclogenesis: case study, *Al-Azhar Bull. Sci*., **11** (1): 35-50.

Abdel Basset, H. and **Gahein, A.** (2003) Diagnostic study on the relation between ozone and potential vorticity, *Atmosfera.*, **16:** 67- 82.

Austin, J., Barwell, B.R., Cox, S.J., Hughes, P.A., Knight, J.R., Ross, G., Sinclair, P. and **Webb, A.R.** (1994) The diagnosis and forecast of clear-sky ultraviolet levels of the Earth's surface, *Meteorol. Appl*., **1:** 321-336.

Berger, D.S. and **Urbach, F.** (1982) A climatology of sun burning ultraviolet radiation, *Photochem. Photobiol*., **35:** 187-192.

Bojkov, R.L., Hill, W. J., Reinsel, G.C. and **Tiao, G.C.** (1990) A statistical trend analysis of revised Dobson total ozone data over the Northern Hemisphere, *J. Geophys. Res.*, **95:** 9785-9807.

Burrows, W.R., Wilson, L.J. and **Vallee, M.** (1993) A Statistical Forecast Procedure for Daily Total Ozone Based on TOMS Data, *13th Conference on Weather Analysis and Forecasting Including Symposium on Flash Floods*, Am. Meteorol. Soc., Vienna, Va., Aug. 2-6.

Burrows, W.R., Vallee, M., Wardle, D.L., Kerr, J.B., Wilson, L.J. and **Tarasick, D.W.** (1994) The Canadian operational procedure for forecasting total ozone and UV radiation, *Meteor. Apps.*, **1:** 247-265.

Dobson, G.M.B., Harrison, D.N. and **Lawrence, J.** (1929) Measurements of the amount of ozone in the Earth's atmosphere and its relation to other geophysical conditions, III, *Proc. R. Soc. London A*., **122:** 456-486.

Frederick, J.E., Koob, A.E., Alberts, A.D. and **Weatherhead, E.C.** (1993) Empirical studies of tropospheric transmission in the ultraviolet: broadband measurements, *J. Appl. Meteor*., **32:** 1883-1892.

Grant, W.B. (1988) Global stratospheric ozone and UV-B radiation, *Science*, **242:** 111.

Mote, P.W., Holton, J.R. and **Wallace, J.M.** (1991) Variability in total ozone associated with baroclinic waves, *J. Atmos Sci*., **48:** 1900-1903.

Normand, C. (1953) Atmospheric ozone and upper air conditions, *Q. J. R. Meteorol. Soc.*, **79:** 39-50.

Ohring, G. and **Muench, H.S.** (1960) Relationships between ozone and meteorological parameters in the lower stratosphere, *J. Meteorol*., **17:** 195-206.

Petzoldt, K., Naujokat, B. and **Neugebohren, K.** (1994) Correlation between stratospheric temperature, total ozone, and tropospheric weather systems, *Geophys. Res. Lett.*, **21:** 1203-1206.

Poulin, I. and **Evans, W.F.J.** (1994) METOZ: Total ozone from meteorological parameters, *Atmos. Ocean*, **32:** 285-297.

Reed, R.J. (1950) The role of vertical motions in ozone-weather relationships, *J. Meteorol*., **7:** 263-267.

Schubert, S.D. and **Munteanu, M.J.** (1988) An analysis of tropopose pressure and total ozone correlation, *Monthly Weather Review*, **116:** 569-582.

Scotto, J., Cotton, G., Urbach, F., Berger, D. and **Fears, T.** (1988) Biologically effective ultraviolet radiation: surface measurements in the United States, 1974 to 1985, *Science*, **239:** 762-764.

Vaughan, G. and **Price, D.J.** (1991) On the relation between total ozone and meteorology, *Q. J. R. Meteorol. Soc.*, **117:** 1281-1298.

Vogel G., Spankuch, D., Schultz, E., Feister, U. and **Dohler, W.** (1995) Regional short-term forecast of total column ozone, *Atmospheric Environment*, **29**(10): 1155-1163.

التنبؤ بالأشعة فوق البنفسجية – ب فوق أسوان

حشمت عبد الباسط محمد و محمد حسين قرني*

كلية الأرصاد والبيئة وزراعة المناطق الجافة – جامعة الملك عبد العزيز
جدة – المملكة العربية السعودية
** الهيئة العامة للأرصاد الجوية – القاهرة – جمهورية مصر العربية*

المستخلص. الهدف الأساسي لهذا البحث هو عمل إجراء للتنبؤ بالأشعة فوق البنفسجية – ب فوق أسوان (٢٣,٩٧ درجة شمالا و ٣٢,٧٨ درجه شرقا). وتعتمد عملية التنبؤ بالأشعة فوق البنفسجية – ب أساسا على إيجاد صيغة رياضية تربط بين الأشعة فوق البنفسجية – ب من جهة والإشعاع الكلي، والكمية الكلية للأوزون فوق أسوان من جهة أخرى. وقد تم عمل التنبؤ للأشعة فوق البنفسجية – ب على ثلاث خطوات: الأولى، تم استنتاج الأوزون فوق أسوان باستنباط معادلة خطية تربط بينه وبين سمك طبقتين من الغلاف الجوي؛ ثانيا، تم استخدام طريقة الباقي لاستنباط صيغة تجريبية تربط بين قيم الإشعاع الكلى ببعض عناصر الأرصاد السطحية؛ وفي النهاية ، تم استخدام قيم الأوزون الكلي وقيم الإشعاع الكلي في صيغة للحصول على توقع لقيم الإشعاع فوق البنفسجي– ب. و طبقت الخطوات السابقة على بيانات فصلية وسنوية. ووجد أن أقوى ارتباط تم الحصول عليه كان في الخريف والشتاء بالنسبة للأوزون، بينما في الربيع والخريف بالنسبة للإشعاع الكلي.